Hindawi Publishing Corporation
Journal of Chemistry
Volume 2016, Article ID 9378460, 11 pages
http://dx.doi.org/10.1155/2016/9378460

Research Article

Performance Investigation of O-Ring Vacuum Membrane Distillation Module for Water Desalination

Adnan Alhathal Alanezi,[1] H. Abdallah,[2] E. El-Zanati,[2] Adnan Ahmad,[3] and Adel O. Sharif[4]

[1]*Department of Chemical Engineering Technology, College of Technological Studies, The Public Authority for Applied Education and Training (PAAET), P.O. Box 117, 44010 Sabah Al-Salem, Kuwait*
[2]*Chemical Engineering and Pilot Plant Department, Engineering Research Division, National Research Centre, Dokki, Giza, Egypt*
[3]*Department of Polymer Engineering and Technology, University of the Punjab, Quaid-e-Azam Campus, P.O. Box 54590, Lahore, Pakistan*
[4]*Qatar Environment and Energy Research Institute, HBKU, Qatar Foundation, Doha, Qatar*

Correspondence should be addressed to Adnan Alhathal Alanezi; aa.alanezi@paaet.edu.kw

Received 14 July 2016; Revised 9 September 2016; Accepted 15 September 2016

Academic Editor: Rosa Maria Gomez Espinosa

A new O-ring flat sheet membrane module design was used to investigate the performance of Vacuum Membrane Distillation (VMD) for water desalination using two commercial polytetrafluoroethylene (PTFE) and polyvinylidene fluoride (PVDF) flat sheet hydrophobic membranes. The design of the membrane module proved its applicability for achieving a high heat transfer coefficient of the order of 10^3 (W/m^2 K) and a high Reynolds number (Re). VMD experiments were conducted to measure the heat and mass transfer coefficients within the membrane module. The effects of the process parameters, such as the feed temperature, feed flow rate, vacuum degree, and feed concentration, on the permeate flux have been investigated. The feed temperature, feed flow rate, and vacuum degree play an important role in enhancing the performance of the VMD process; therefore, optimizing all of these parameters is the best way to achieve a high permeate flux. The PTFE membrane showed better performance than the PVDF membrane in VMD desalination. The obtained water flux is relatively high compared to that reported in the literature, reaching 43.8 and 52.6 (kg/m^2 h) for PVDF and PTFE, respectively. The salt rejection of NaCl was higher than 99% for both membranes.

1. Introduction

Fresh water shortages and water scarcity are major global issues, especially in the arid and semiarid regions of the world, where fresh water can be obtained through different techniques, such as the desalination of seawater. Desalination is one of the earliest methods known to man of obtaining salt-free water. In nature, it forms the source of the hydrological cycle. Desalination usually refers to the process of reducing the concentration of salt and dissolved substances in seawater or brackish water to make it palatable and suitable for consumption. In addition to salt removal, some desalination techniques also remove suspended material, organic matter, bacteria, and viruses [1–5]. Desalination has great potential for supplying fresh water for the 2.4 billion people living in coastal areas, which is equivalent to 39% of the world population. As a result, over the past 15 years, the daily water production has increased from approximately 13 million m^3/day to the current 48 million m^3/day in the 17,000 desalination plants operating worldwide [6]. Globally, more than 80% of the world's desalination capacity is provided by two processes: multistage flash (MSF) and reverse osmosis (RO) [7]. However, these technologies are energy intensive, with the energy mainly supplied by fossil fuel sources, and are not linked to renewable energy sources. Among the recent technologies, membrane distillation (MD) has the advantage of performing at moderate temperatures and pressure [2, 3, 8, 9]. MD process is an emerging thermally driven membrane process and can be applied successfully in desalination [10, 11]. The MD process is economical in terms of energy because the heat source for the process can be low grade and/or alternative energy sources such as solar and geothermal energy and because energy is continuously recovered [2, 8, 9, 12]. During the MD process, a hot saline solution is brought

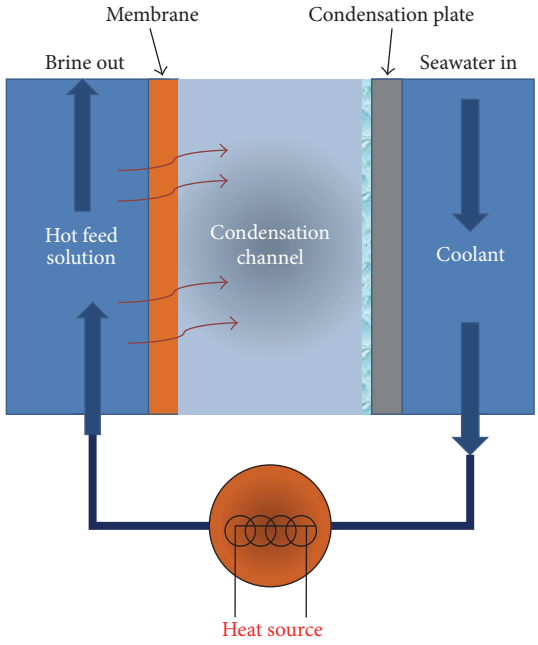

Figure 1: Principle of the membrane distillation (MD) process.

in contact with a hydrophobic membrane, which allows water vapor to diffuse through the membrane, restricting the flow of liquid and hence dissolved salts through its pores [13, 14]. The mass transfer of water vapor through the membrane pores is facilitated by the vapor pressure difference, as well as the temperature difference between the two sides of the hydrophobic membrane, that is, the feed side and the permeate side, as shown in Figure 1 [2, 3, 8, 14–16]. MD can be divided into four configurations (Figure 2) such as (a) Direct Contact Membrane Distillation (DCMD), where the membrane is in direct contact with the cold and hot fluids, (b) Air Gap Membrane Distillation (AGMD), where an air gap is introduced between the membrane and the condensation surface, (c) Sweeping Gas Membrane Distillation (SGMD), where a cold inert gas is employed to sweep the water vapor at the permeate side to condense outside the membrane module, and (d) Vacuum Membrane Distillation (VMD), where the vacuum is applied to the permeate side by means of a vacuum pump to condense the water vapor outside of the membrane module [2, 9, 10, 17]. The difference between these configurations depends on the way in which the vapor is condensed and/or removed from the membrane module [2]. All four configurations have advantages and disadvantages, depending on their applications with the feed solution to be treated [2, 3, 16, 18]. VMD process has many attractive features compared to other MD configurations, where one of the greatest advantages of the VMD process is that heat conduction across the membrane is negligible due to the very low pressure (i.e., a high vacuum degree) on the permeate side; therefore VMD is highly efficient in terms of energy [2, 19]. Additionally, the low pressure enables the VMD process to achieve the best performance in terms of permeate flux compared to other MD configurations [2, 20]. The mechanism makes the VMD process appropriate for separation of various volatile compounds from their aqueous solutions or a mixture of the same and it is only recently that it was applied for seawater desalination and treatment of RO brines [21, 22] However, VMD process has attracted less attention compared to other MD processes and few papers have focused on the fabrication of membranes modules for VMD applications [22–33]. Therefore, in our previous study, new asymmetric PES/TiO_2NTs (polyethersulfone blends with titanium dioxide nanotubes) blend membranes were successfully fabricated by the phase inversion method. The results showed a significant improvement in the performance of the new membrane compared to the commercial membrane, where the permeate flux and salt rejection reached 5.5 (kg/m^2 h) and 96.7% at 35,000 ppm, respectively [34]. Due to the advantages of the VMD process, the new O-ring membrane module was designed and developed. Therefore, the main objective of this paper is to investigate the effect of the operating conditions such as feed temperature, feed flow rate, vacuum degree, and feed concentration using the O-ring membrane module on the performance of VMD process for two commercial PTFE and PVDF hydrophobic membranes.

2. Experimental Work

2.1. Flat Sheet Membrane Modules. A flat sheet O-ring membrane module was designed and specially manufactured to apply Vacuum Membrane Distillation to seawater desalination (Figure 3). The O-ring membrane module consists of three opening holes, one for controlling the vacuum on the permeate side and the other two for feed and water recycling to the feed tank, where the membrane module was constructed to provide better mixing, which increases the heat and mass transfer coefficients and consequently enhances the performance of the VMD process.

2.2. Experimental Set-Up. The experiments were carried out on a bench scale unit, as shown in Figure 4. The feed solution was continuously fed into the membrane module from the feed tank using a peristaltic feed pump. The feed solution was heated using a hot plate, and the feed temperature T_f (28–65°C) was controlled by a hot plate thermostat and recorded using a thermometer. The flow rates used (27.7, 58.7, 97.2, and 110.2 L/h) were measured by a flow meter connected to the feed pump. Vacuum or low pressure on the permeate side P_p (Pa) was obtained using a vacuum pump. The condenser was designed in an efficient manner in which the water vapor was transferred and drawn through the membrane pores to the condenser and then condensed in a condenser jacket using cooling water. The cooling water was fed and recycled continuously using a peristaltic pump into the condenser jacket with a constant cooling temperature of 5°C. The permeate was collected downstream of the condenser.

2.3. Experimental Procedures. Two commercial hydrophobic microporous flat sheet PTFE and PVDF membranes (Fluoropore, Millipore) were used in this experiment. Their

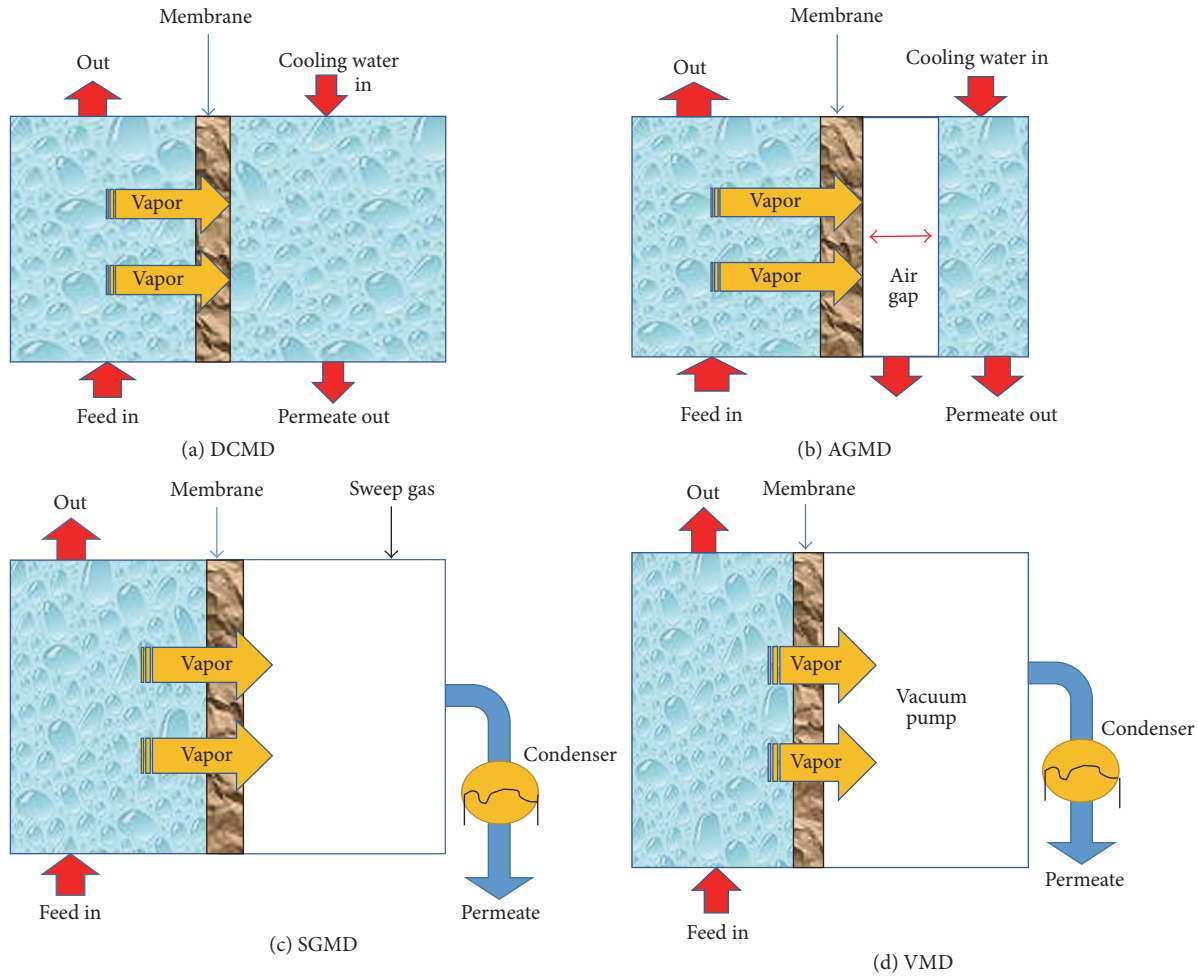

Figure 2: The membrane distillation configurations.

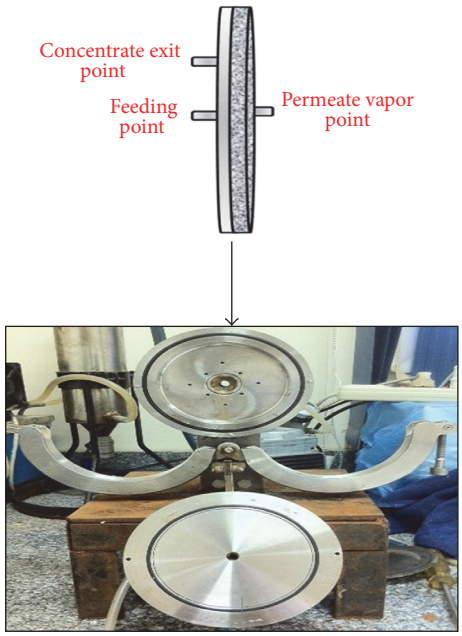

Figure 3: O-ring membrane module.

characteristics are shown in Table 1. The membrane effective area was 117 cm^2. A synthetic salt solution was prepared at different concentrations using commercial sodium chloride (NaCl). Cold water was used to cool the condenser. The feed solutions and permeate solutions were measured using a conductivity meter. The performance of the VMD process in terms of the water flux and salt rejection was investigated for both membranes at different feed temperatures (28, 45, 55, and 65°C), feed flow rates (27.7, 58.7, 97.2, and 110.2 L/h), feed concentrations (10,000, 20,000, and 35,000 mg/L), and vacuum degrees (92, 94, 96, and 97 kPa). During the experiments, the water flux was measured every 15 minutes, where each run lasted for 3 hours and the water flux for each experimental run was the mean value of the fluxes computed in steady state operation with an experimental error of less than 5%. The water flux was calculated using the following formula:

$$J_m = \frac{V}{(A_m t)}, \quad (1)$$

where J_m is the water flux (kg/m^2 h), V is the collected sample volume (L), A_m is the membrane effective area (m^2), and t is the running time (h).

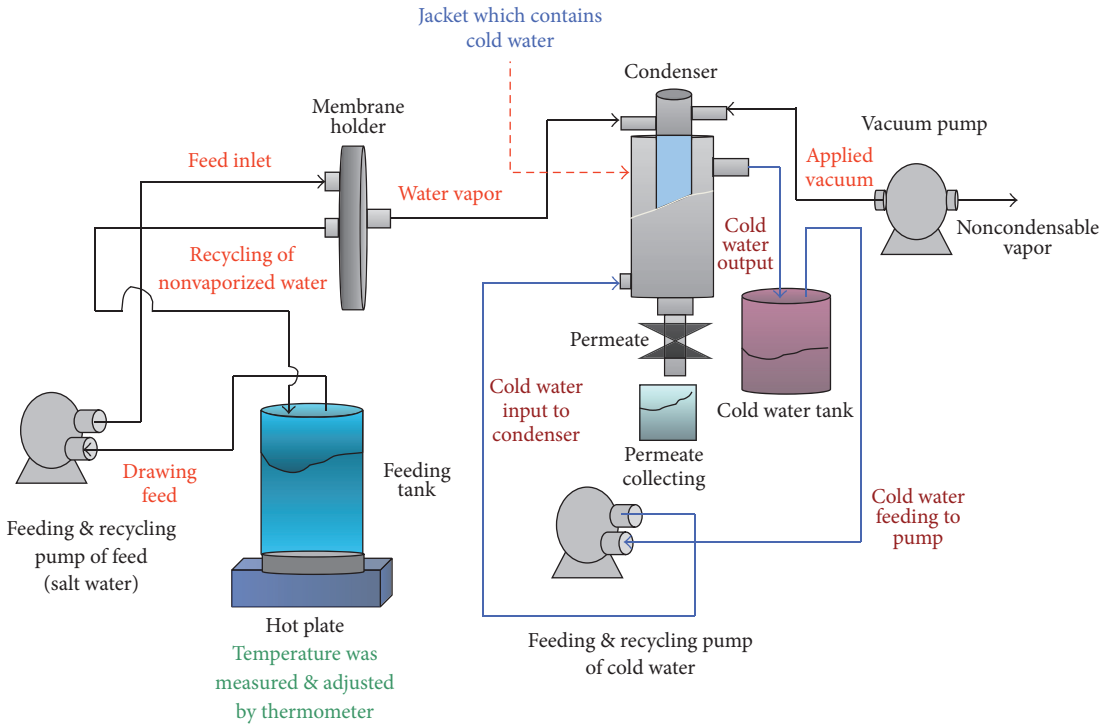

Figure 4: VMD experimental set-up.

Table 1: Membrane properties.

Membrane type	PTFE	PVDF
Pore size (μm)	0.2	0.22
Porosity %	75	75
Thickness (μm)	120	200
Thermal conductivity (W/m·K)	0.28	0.20

3. Results and Discussion

3.1. VMD Experiments for Pure and Saline Water. A series of pure water and saline water (35,000 mg/L) VMD experiments were conducted using two commercial PTFE and PVDF hydrophobic membranes to evaluate the fluid dynamics at the feed boundary layer, where the experimental results were used to evaluate the constant parameters (a and b) of the heat and mass transfer analogy. Pure and saline water were kept in turbulent flow in the membrane module to calculate the heat (h_f) and mass (k_f) transfer coefficients, respectively, from the obtained correlations. A dimensionless Nusselt number (Nu) is commonly used to relate h_f to other factors that affect heat transfer in the feed boundary layer, as illustrated in the equation below:

$$\mathrm{Nu} = \frac{h_f d}{k} = a\,\mathrm{Re}^b\,\mathrm{Pr}^c. \tag{2}$$

$$\log\frac{\mathrm{Nu}}{\mathrm{Pr}^c} = \log a + b\log \mathrm{Re}. \tag{3}$$

The exponent of the Prandtl number (Pr) c is usually equal to 1/3. Therefore, to determine a and b, some of the experimental results with pure water for the two membranes are listed in Table 2. The water flux J_m was measured under various feed flow rates F_f (27.7 to 110.2 L/h), a constant feed temperature T_f (65°C), and vacuum degree levels (92 kPa). As shown in Table 2, the Reynolds number within the membrane module lies in the turbulent flow region, and the Prandtl number is constant (2.77) at 65°C. Figures 5(a) and 5(b) show the results of a straight line equation plotted as $\log \mathrm{Nu}/\mathrm{Pr}^{1/3}$ versus $\log \mathrm{Re}$ for pure and saline water, respectively, where the intercept is equal to $\log a$ and the slope is equal to b, as shown in (3). It is obvious from Figures 5(a) and 5(b) that the value of intercept b is equal to 0.81 and 0.82 and the values of a are $10^{-1.7184}$ and $10^{-1.7277}$, which are equal to 0.0191 and 0.0187, respectively. Therefore, (2) and (3) can be written as shown in (4) and (5). Consider

$$\mathrm{Nu} = \frac{h_f k}{d} = 0.0191\,\mathrm{Re}^{0.81}\,\mathrm{Pr}^{(1/3)}\ \text{Pure water}. \tag{4}$$

$$\mathrm{Nu} = \frac{h_f k}{d} = 0.0187\,\mathrm{Re}^{0.82}\,\mathrm{Pr}^{(1/3)}\ \text{saline water}\,(35{,}000\ \mathrm{mg/L}). \tag{5}$$

Therefore, using (3) and (4), the heat transfer coefficient h_f can be obtained, and because the heat and mass transfer are involved simultaneously in VMD, the mass transfer coefficient k_f on the feed side can be calculated using the equation shown below:

$$\frac{h_f}{k_f} = \frac{k_L}{D_{\mathrm{AB}}\,(\mathrm{Pr}/\mathrm{Sc})^{1/3}}. \tag{6}$$

Table 2: Pure water VMD experimental results for PVDF and PTFE at a 92 kPa vacuum degree.

Run	T_f (°C)	v_f (m/s)	J_m (kg/m^2 h)		h_f (W/m^2 K)	$k_f \times 10^{-2}$	Re	Nu	Pr
			PVDF	PTFE					
1	65	0.32	17.7	19.4	1553.8	3.97	86711.31	288.2	2.77
2	65	0.67	35.7	37.7	2821.6	7.23	183557.7	523.2	2.77
3	65	1.11	53.1	58.9	4225.0	10.83	304052.6	783.5	2.77
4	65	1.25	55.2	63.8	4670.0	11.97	344593.0	866.0	2.77

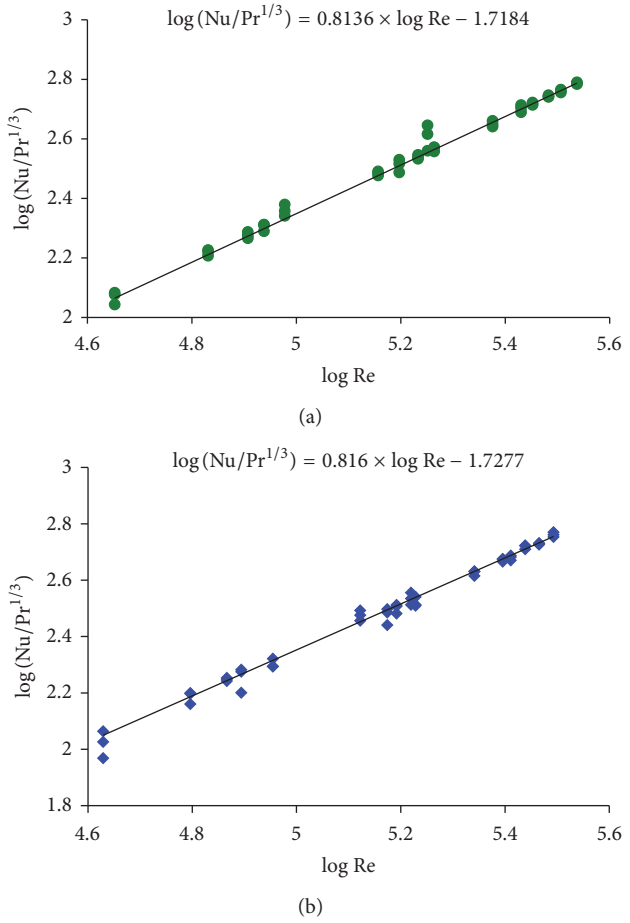

Figure 5: The linear relationship of log(Nu/Pr$^{1/3}$) versus log(Re) for the (a) pure and (b) saline water.

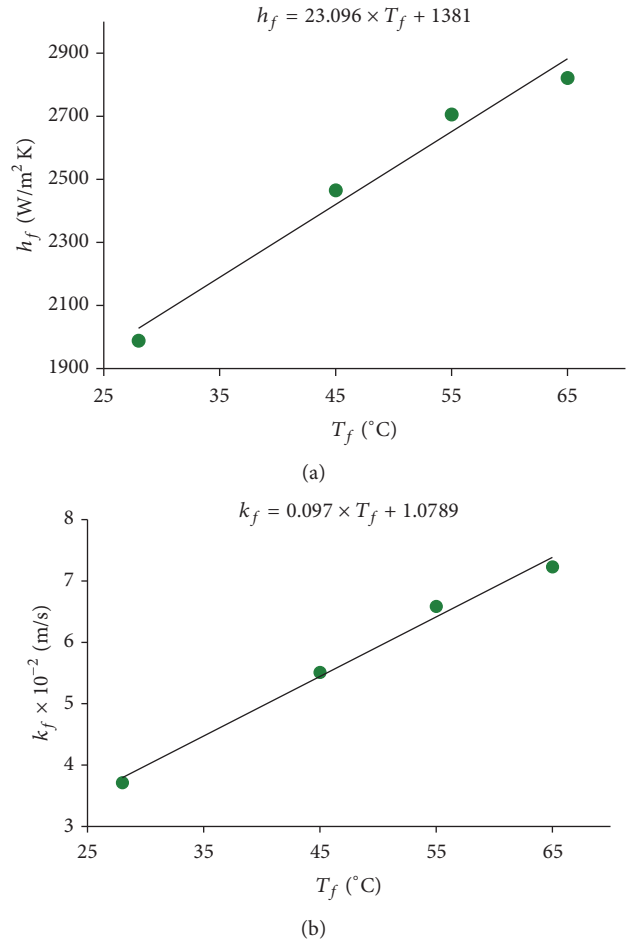

Figure 6: The pure water (a) heat (h_f) and (b) mass (k_f) transfer coefficients versus the feed temperature at a flow rate of 58.7 L/h.

The linear relationship of the heat (h_f) and mass (k_f) transfer coefficients of the membrane module versus the feed temperature T_f for pure and saline water at 58.7 L/h is shown in Figures 6(a) and 6(b) and Table 3, respectively.

Table 3: Derived heat and mass transfer coefficients of saline water.

NaCl concentration, C_f (mg/L)	h_f (W/m^2 K)	$k_f \times 10^{-2}$ (m/s)
10,000	$22.335T_f + 1396.9$	$0.0936T_f + 1.130$
20,000	$21.656T_f + 1398.9$	$0.0903T_f + 1.177$
35,000	$20.679T_f + 1400.8$	$0.0856T_f + 1.242$

3.1.1. VMD Performance. The performance of VMD in terms of its water flux and salt rejection has been studied experimentally by investigating the effects of various operating parameters, such as the feed temperature, feed flow rate, vacuum degree, and NaCl concentration in the feed.

(1) Effect of Feed Temperature. The effect of the feed temperature on the permeate flux of the PVDF and PTFE membranes was studied under different feed flow rate conditions (27.7, 58.7, 97.2, and 110.2 L/h) and a constant vacuum degree (97 kPa) and feed concentration (35,000 mg/L). As shown in Figures 7(a) and 7(b), the feed temperature had a remarkable

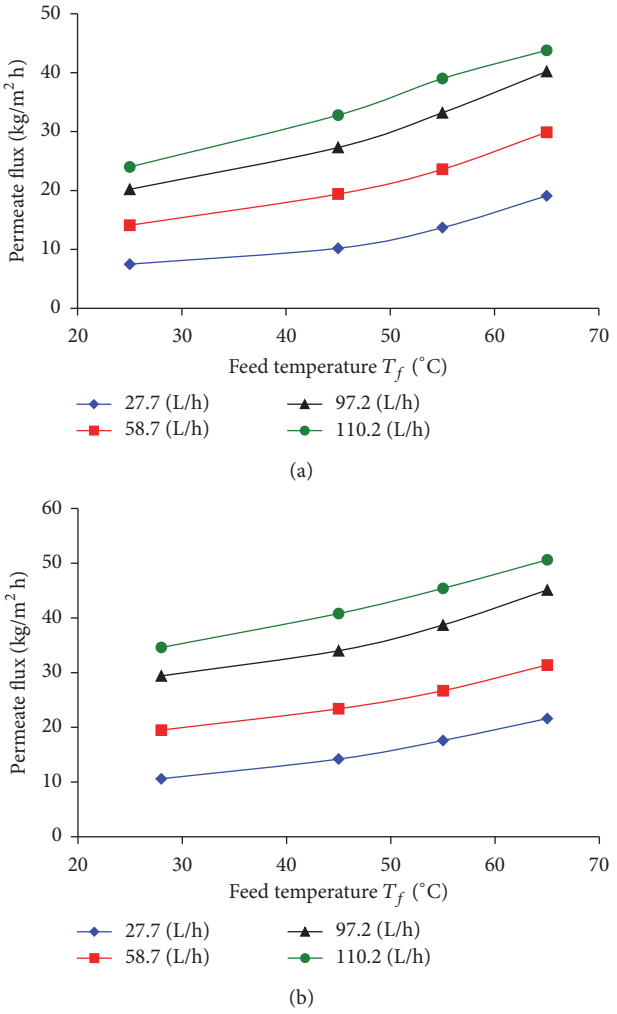

Figure 7: The effect of the feed temperature on the permeate flux through (a) PVDF and (b) PTFE membranes at different feed flow rates, with 97 kPa vacuum degree and feed concentration of 35,000 mg/L.

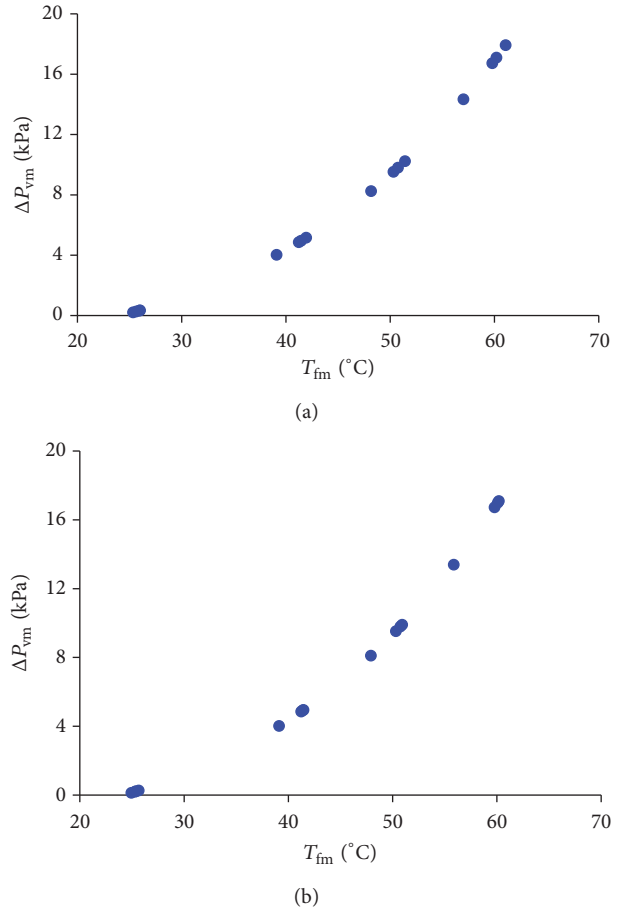

Figure 8: The variations in the membrane surface temperature T_{fm} with the vapor pressure difference ΔP_{vm} for the (a) PVDF and (b) PTFE membranes.

influence on the water flux of VMD. As expected, the water flux of VMD for both membranes increases exponentially with the feed temperature. This is due to the major effect of temperature on the water vapor pressure according to the exponential Antoine equation [2, 8, 34]. Increasing the feed temperature decreases the feed viscosity and the thickness of the boundary layer, which significantly enhances the mass transfer coefficient. Furthermore, as shown in Figures 8(a) and 8(b), increasing the feed temperature (T_f) can significantly increase the membrane surface temperature (T_{fm}), which consequently increases the vapor pressure difference ΔP_{vm} across the membrane module and therefore enhances the water flux of VMD, where the feed surface temperature T_{fm} and vapor pressure difference ΔP_{vm} are calculated based on the experimental data for different feed temperatures, feed flow rates, and vacuum levels. For instance, increasing the feed temperature from 28 to 65°C at 110.2 (L/h) increases the VMD water flux from 24 to 45.8 (kg/m^2 h) for PVDF and 34.6 to 52.6 (kg/m^2 h) for PTFE. It is clear that the PTFE membrane provides a much higher water flux than the PVDF membrane. This is mainly due to the difference in membrane thickness (200 μm for PVDF and 120 μm for PTFE) where the thin membrane has a lower resistance to mass transfer across it.

(2) Effect of the Feed Flow Rate. The feed flow rate is also one of the most important parameters that affect the performance of the VMD process. The effect of the feed flow rate on the water flux was investigated for the PVDF and PTFE membranes by changing it from 27.7 to 110.2 (L/h) for different vacuum levels (92, 94, 96, and 97 kPa) at a constant feed concentration of 35,000 mg/L and feed temperature of 65°C. The changes in the VMD water flux for both membranes with respect to the various feed flow rates are shown in Figures 9(a) and 9(b), respectively. It is obvious that the permeate flux of VMD increases rapidly for both membranes with an increasing feed flow rate. This increase is due to the increase in Reynolds number, which causes enhanced mixing of the flow in the channels due to the turbulence. In other words, the enhanced turbulent flow reduces the thickness of the boundary layers for both the temperature and concentration

Table 4: The effect of the feed flow rate on the heat transfer coefficient, surface temperature, and temperature polarization coefficient at 55 and 65°C and a constant vacuum level of 92 kPa.

Feed flow rate (F_f) (mL/s)	Re	55°C			65°C		
		h_f (W/m^2 K)	T_{fm} (°C)	TPC	h_f (W/m^2 K)	T_{fm} (°C)	TPC
7.7	78315	1420.1	51.7	0.94	1475.6	60.7	0.93
16.6	165784	2587.5	52.3	0.95	2688.6	61.3	0.94
27	274612	3874.5	52.7	0.96	4026.0	61.6	0.95
30.3	311226	4282.5	53.2	0.97	4450.0	62.0	0.96

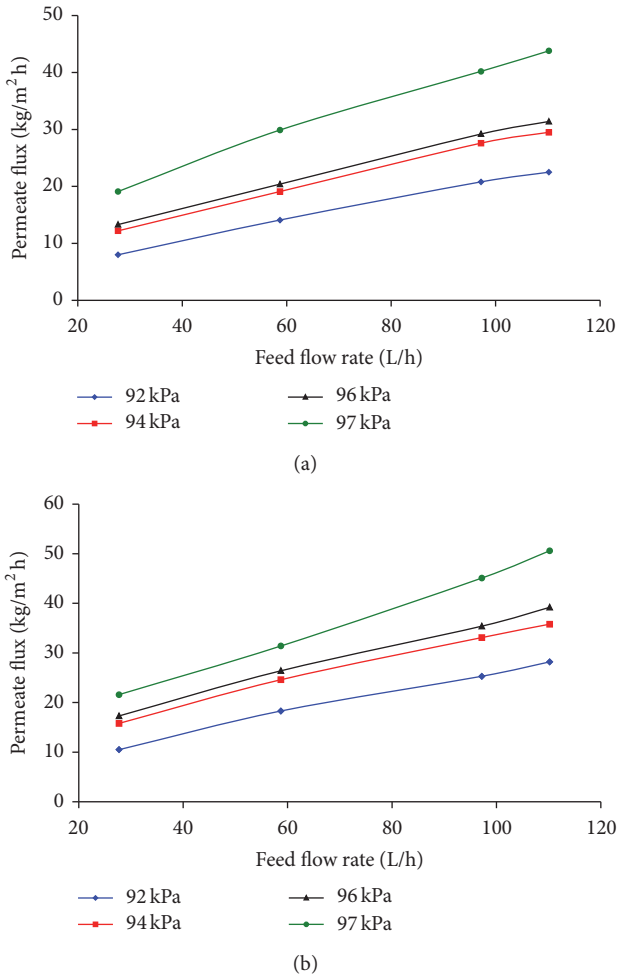

Figure 9: The effect of the feed flow rate on the permeate flux of (a) PVDF and (b) PTFE membranes at different vacuum degrees, with a feed temperature of 65°C and feed concentration of 35,000 mg/L.

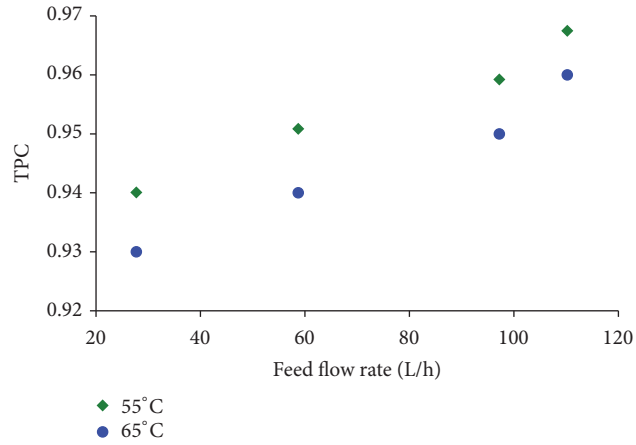

Figure 10: The effect of the feed flow rate on the temperature polarization coefficient at a constant 92 kPa vacuum degree and feed temperatures of 55 and 65°C.

(i.e., the boundary layer resistance), which consequently increases the driving force for evaporation. Moreover, the turbulence increases the convective heat transfer coefficient h_f at the feed boundary layer. This is clear from (3) and (4), where h_f is directly proportional to $\mathrm{Re}^{0.8}$, which consequently speeds up the heat transfer process from the bulk feed to the membrane surface [20, 38, 39]. This consequently increases the feed membrane surface temperature T_{fm} and temperature polarization coefficient (TPC), as seen in Table 4 and Figure 10, respectively. The TPC clearly increases with the increasing feed flow rate; this is due to the reduction of the heat transfer resistance within the boundary layers. However, the feed temperature has a negative influence on the TPC. This is attributed to the increased heat flux through the thermal boundary layer, which leads to a decrease in the membrane surface temperature T_{fm} [40]. Thus, increasing the feed flow rate is one way to mitigate the temperature polarization effect in VMD. Additionally, the increase in water flux seemed to approach the maximum values asymptotically with a higher feed flow rate [41–43]; for example, in Figure 9(a), the percentage increase in the water flux from 27.7 to 58.7 (L/h) was 57%, while it decreased to 9% from 97.2 to 110.2 (L/h). Therefore, a further increase in Reynolds number has less effect on the water flux so that the effective method is to optimize the feed flow rate to reach a high water flux [41, 44]. The results from Figures 9(a) and 9(b) show that the PTFE membrane provides a higher flux compared to the PVDF membrane, where the PTFE membrane reached a permeate flux of 50.6 (kg/m^2 h) at 65°C and 97 kPa vacuum degree, while the flux was 43.8 (kg/m^2 h) for the PVDF membrane under the same conditions.

(3) Effect of the Vacuum Degree. Based on some studies [35, 45], the vacuum degree on the permeate side was one of the most significant factors, along with the feed temperature and feed flow, which affect the performance of the VMD

Table 5: Heat flux for evaporation at different vacuum degrees for the PVDF and PTFE membranes.

Feed flow rate (F_f) (mL/s)	Heat flux, Q (W), PVDF vacuum degree kPa at 65°C				Heat flux, Q (W), PTFE vacuum degree kPa at 65°C			
	92	94	96	97	92	94	96	97
7.7	74.2	64.5	103.2	125.8	80.6	122.5	132.2	161.2
16.3	116.0	116.0	163.8	184.3	136.5	191.2	204.8	245.7
27.0	158.3	158.3	226.1	260.1	192.2	260.1	271.4	328.0
30.6	153.8	179.4	294.7	346.0	217.8	333.2	346.0	410.1

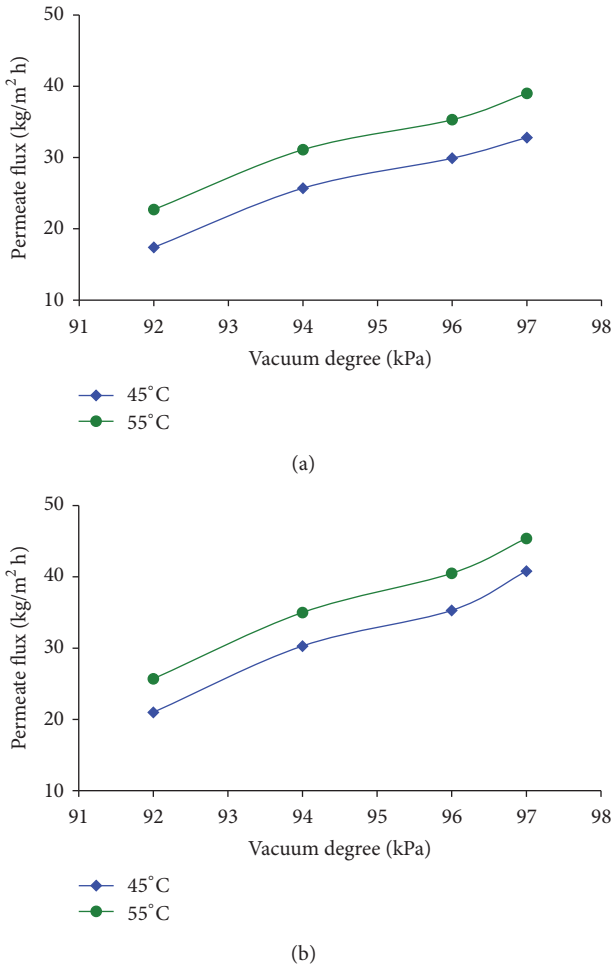

Figure 11: The effect of the vacuum degree on the permeate flux at 45 and 55°C feed temperatures; 110.2 (L/h) feed flow rate and 35,000 mg/L of NaCl for (a) PVDF and (b) PTFE membranes.

process. In Figures 11(a), 11(b), 12(a), and 12(b), the water flux was plotted as a function of the vacuum degree at a 35,000 mg/L feed concentration, different feed temperatures, and feed flow rates. As shown in Figures 11(a), 11(b), 12(a), and 12(b), increasing the vacuum degree, while varying the feed temperature and feed flow rate, causes the water flux to increase linearly. This is attributed to the significant decrease in water vapor pressure on the permeate side, consequently enhancing the vapor pressure difference (i.e., the driving force) through the membrane; it is clear from the curve behavior that the effect of the feed temperature with the vacuum degree is more significant than the effect of the feed flow rate with the vacuum [26, 29, 46–48]. This is because the vapor pressure difference across the membrane is induced by the temperature at the feed side and the high vacuum applied to the permeate side. In addition, the percentage increase in the water flux when the vacuum level was first changed (i.e., from 92 to 94 kPa) increases dramatically at various feed temperature and feed flow rates, but the percentage increase is reduced as the vacuum level increases from 96 to 97 kPa. For example, at 27.7 (L/h) and 55°C, the water flux increased from 5.6 to 9.8 (kg/m^2 h), that is, by more than 75%, while the percentage increase was 15% for a change in the vacuum degree from 96 to 97 kPa. This means that the increase in water flux is reduced as the vacuum degree increases with the feed temperature and feed flow rate. Therefore, there is a trade-off between all of these variables in their effect on VMD performance; therefore, optimizing all of them is the best way to achieve a high water flux. Moreover, as shown in Table 5, increasing the vacuum level increases the amount of heat flux required for evaporation, which is consequently necessary for increasing the performance of the VMD process. For example, the increase in the heat flux for the PVDF membrane from a 92 kPa vacuum degree to that of 97 kPa at a feed flow rate of 110.2 (L/h) and feed temperature of 65°C is greater than a twofold increase. The water flux of the PTFE membrane is higher than that of the PVDF membrane under the same operating conditions of the feed temperature and feed flow rate, where the water flux through the PTFE membrane is 13–16% greater than that for the PVDF membrane.

(4) Effect of the Feed Concentration. The effect of the feed concentration of the NaCl salt in aqueous solutions on the water flux and percentage rejection was investigated in VMD. The experiments were performed for different feed concentrations (10,000, 20,000, and 35,000 mg/L) where the feed temperature, the feed flow rate, and the vacuum degree were kept constant at 65°C, 58.7 (L/h), and 97 kPa, respectively. From Figure 13, the effect of the feed concentration of NaCl on the water flux may be noted. The results show that the water flux decreases as the NaCl concentration increases due to the reduction of the vapor pressure difference, which decreases the amount of water vapor flowing across the membrane. Furthermore, Alhathal et al. and Mericq et al. [8, 21] attributed the decline in the permeate flux to the variation in the NaCl thermodynamic properties (i.e., the water activity coefficient). Moreover, the temperature and

Table 6: Comparison of the PVDF and PTFE membranes at 65°C, 110.2 (L/h), and 97 kPa for 35 g/L.

Membrane	Permeate flux (kg/m^2 h)	Permeate concentration (mg/L)	Permeate conductivity (μS/cm)	% of rejection
PVDF	43.8	175	8.1	99.5
PTFE	52.6	280	10.2	99.2

Table 7: Comparison of the permeate fluxes at different operating conditions in MD for different NaCl solutions.

MD type	Membrane	d_p (μm)	T_f (°C)	Vacuum (kPa)	F_f (mL/s)	C_f (g/L)	Flux (kg/m^2 h)	Ref.
VMD	PTFE	0.1	65	100	2280	35	66	[19]
VMD	PP 50/200	0.1	90	87	5 cm/s	3.5	15	[29]
VMD	PES/TiO_2NTs	—	65	70	11	35	5.5	[34]
VMD	PP	0.2	55	97	30	100	14.4	[35]
VMD	PP	0.074	60	93	42	35	3	[36]
VMD	PVDF	0.2	60	14.5	25	3.5	4	[37]
VMD	PVDF	0.22	65	97	30.6	35	43.8	This study
VMD	PTFE	0.22	65	97	30.6	35	52.6	This study

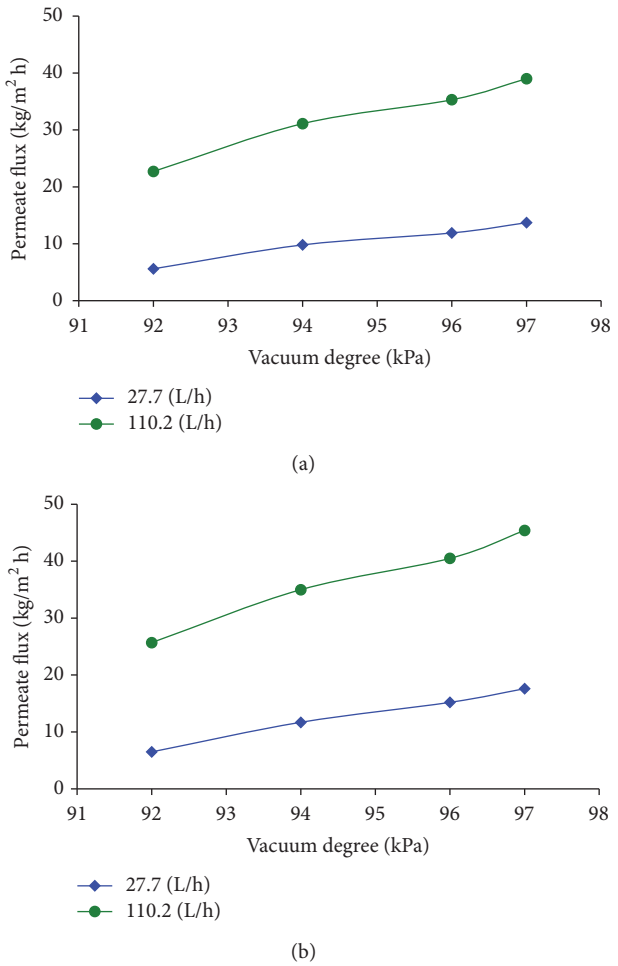

Figure 12: The effect of the vacuum degree on the permeate flux at 27.7 and 110.2 (L/h) feed flow rates; a 55°C feed temperature and 35,000 mg/L of NaCl for the (a) PVDF and (b) PTFE membranes.

concentration polarization effects reduce the evaporation driving force where the thickness of the boundary layer is increased. As the concentration increases from 10,000 mg/L to 35,000 mg/L, the decline in flux is 14% for PTFE and 15% for PVDF, while the percentage rejection of salt shows more than 99% for both membranes. Based on previous studies [13, 34], MD process can treat a highly saline water at a feed concentration of 35,000 to 180,000 (mg/L), with a decline in water flux from 13 to 35%, while the salt rejection is not affected by the feed concentration.

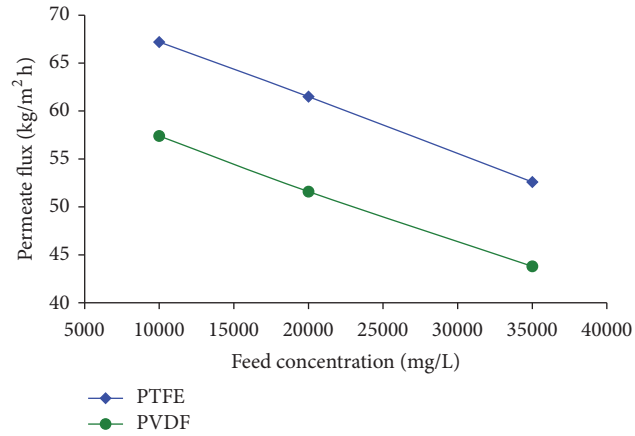

Figure 13: The effect of the feed concentration of NaCl on the permeate flux for PTFE and PVDF membranes at a 65°C feed temperature, 110.2 (L/h) feed flow rate, and 97 kPa vacuum degree.

(5) Comparison of the PVDF and PTFE Membranes. Within the investigation, a range of experimental operating conditions of a 65°C feed temperature, 110.2 (L/h) feed flow rate, and 97 kPa vacuum degree at a feed concentration of 35,000 (mg/L) was chosen for comparison with previous studies of VMD in terms of water flux, water quality, and salt rejection, as shown in Tables 6 and 7. It is clear that the water fluxes and salt rejection were 43.8 (kg/m^2 h) and 99.5% for PVDF and 52.6 (kg/m^2 h) and 99.2% for PTFE. In terms of water quality, the average electrical conductivities of the permeates are 8.1 and 10.2 μS/cm for the PVDF and PTFE membranes, respectively.

4. Conclusions

An O-ring membrane module was constructed and specially designed to investigate the performance of the VMD process using PTFE and PVDF membranes. Pure water experiments were conducted to measure the heat and mass transfer coefficients within the membrane module. The results were used to reevaluate the constant parameters of the heat and mass transfer analogy. Therefore, the obtained equations were used to calculate the heat and mass transfer coefficients. The results showed that the membrane module design proved its applicability for achieving a high heat transfer coefficient h_f of the order of 10^3 (W/m^2 K) and high Reynolds number (Re). The effect of process parameters, namely, the feed temperature, feed flow rate, vacuum degree, and feed concentration, on the performance of VMD process in terms of water flux and salt rejection has been discussed. The results showed that the water flux increased exponentially with feed temperature. Additionally, the water flux increased with the increasing feed flow rate and seemed to approach maximum values asymptotically at higher flow rates. The degree of vacuum plays an important role in increasing the process performance, where the water flux increases linearly with an increasing vacuum degree. Therefore, there is a trade-off between these three variables on the effect of the VMD performance, so optimizing all of them is the best way to achieve a high permeate flux. As expected, the feed concentration of 10,000 to 35,000 mg/L of NaCl decreased the water flux, where the percentage decline was approximately 13 and 14% for PTFE and PVDF, respectively. It was concluded that, at operating conditions of a 65°C feed temperature, 110.2 (L/h) feed flow rate, and 97 kPa vacuum degree for a 35,000 (mg/L) feed concentration, the water flux reached 43.8 and 52.6 (kg/m^2 h) for PVDF and PTFE, respectively, and the salt rejection of NaCl was higher than 99% for both membranes. Within the investigation range of the experimental operating conditions, the obtained water fluxes were relatively high compared to those reported in the literature, and these results might be attributed to the unique design of O-ring membrane module and the condenser.

Competing Interests

The authors declare that they have no competing interests.

Acknowledgments

The authors wish to express their sincere thanks to the Public Authority of Applied Education and Training (PAAET) in Kuwait for funding this research.

References

[1] A. Altaee, "Forward osmosis: potential use in desalination and water reuse," *Journal of Membrane and Separation Technology*, vol. 1, pp. 79–93, 2012.

[2] A. AlHathal Al-Anezi, A. O. Sharif, M. I. Sanduk, and A. R. Khan, "Potential of membrane distillation—a comprehensive review," *International Journal of Water*, vol. 7, no. 4, pp. 317–346, 2013.

[3] A. A. Alanezi and A.O. Sharif, "Membrane distillation: an attractive alternative," *Arab Water World*, vol. 36, no. 5, pp. 1–77, 2012.

[4] H. T. El-Dessouky and H. M. Ettouney, *Fundamentals of Salt Water Desalination, Department of Chemical Engineering, College of Engineering and Petroleum, Kuwait University*, Elsevier, Amsterdam, Netherlands, 2002.

[5] A. Ahmad, F. Jamshed, T. Riaz et al., "Self-sterilized composite membranes of cellulose acetate/polyethylene glycol for water desalination," *Carbohydrate Polymers*, vol. 149, pp. 207–216, 2016.

[6] R. Gemma Raluy, R. Schwantes, V. J. Subiela, B. Peñate, G. Melián, and J. R. Betancort, "Operational experience of a solar membrane distillation demonstration plant in Pozo Izquierdo-Gran Canaria Island (Spain)," *Desalination*, vol. 290, pp. 1–13, 2012.

[7] M. A. Eltawil, Z. Zhengming, and L. Yuan, "A review of renewable energy technologies integrated with desalination systems," *Renewable and Sustainable Energy Reviews*, vol. 13, no. 9, pp. 2245–2262, 2009.

[8] A. A. Al-Anezi, A. O. Sharif, M. I. Sanduk, and A. R. Khan, "Experimental investigation of heat and mass transfer in tubular membrane distillation module for desalination," *ISRN Chemical Engineering*, vol. 2012, Article ID 738731, 8 pages, 2012.

[9] M. Khayet, "Solar desalination by membrane distillation: dispersion in energy consumption analysis and water production costs (a review)," *Desalination*, vol. 308, pp. 89–101, 2013.

[10] M. M. A. Shirazi, A. Kargari, and M. Tabatabaei, "Evaluation of commercial PTFE membranes in desalination by direct contact membrane distillation," *Chemical Engineering and Processing: Process Intensification*, vol. 76, pp. 16–25, 2014.

[11] L. Martínez, "Comparison of membrane distillation performance using different feeds," *Desalination*, vol. 168, no. 1–3, pp. 359–365, 2004.

[12] L. M. Camacho, L. Dumée, J. Zhang et al., "Advances in membrane distillation for water desalination and purification applications," *Water*, vol. 5, no. 1, pp. 94–196, 2013.

[13] A. Alkhudhiri, N. Darwish, and N. Hilal, "Produced water treatment: application of air gap membrane distillation," *Desalination*, vol. 309, pp. 46–51, 2013.

[14] H. C. Duong, A. R. Chivas, B. Nelemans et al., "Treatment of RO brine from CSG produced water by spiral-wound air gap membrane distillation—a pilot study," *Desalination*, vol. 366, pp. 121–129, 2015.

[15] A. S. Alsaadi, N. Ghaffour, J.-D. Li et al., "Modeling of air-gap membrane distillation process: a theoretical and experimental study," *Journal of Membrane Science*, vol. 445, pp. 53–65, 2013.

[16] S. Al-Obaidani, E. Curcio, F. Macedonio, G. Di Profio, H. Al-Hinai, and E. Drioli, "Potential of membrane distillation in seawater desalination: thermal efficiency, sensitivity study and cost estimation," *Journal of Membrane Science*, vol. 323, no. 1, pp. 85–98, 2008.

[17] P. Wang and T.-S. Chung, "Recent advances in membrane distillation processes: membrane development, configuration design and application exploring," *Journal of Membrane Science*, vol. 474, pp. 39–56, 2015.

[18] E. Curcio and E. Drioli, "Membrane distillation and related operations—a review," *Separation and Purification Reviews*, vol. 34, no. 1, pp. 35–86, 2005.

[19] J. P. Mericq, S. Laborie, and C. Cabassud, "Vacuum membrane distillation for an integrated seawater desalination process," *Desalination and Water Treatment*, vol. 9, no. 1–3, pp. 293–302, 2009.

[20] M. S. El-Bourawi, Z. Ding, R. Ma, and M. Khayet, "A framework for better understanding membrane distillation separation process," *Journal of Membrane Science*, vol. 285, no. 1-2, pp. 4–29, 2006.

[21] J.-P. Mericq, S. Laborie, and C. Cabassud, "Vacuum membrane distillation of seawater reverse osmosis brines," *Water Research*, vol. 44, no. 18, pp. 5260–5273, 2010.

[22] S. Cerneaux, I. Struzyńska, W. M. Kujawski, M. Persin, and A. Larbot, "Comparison of various membrane distillation methods for desalination using hydrophobic ceramic membranes," *Journal of Membrane Science*, vol. 337, no. 1-2, pp. 55–60, 2009.

[23] Z. Jin, D. L. Yang, S. H. Zhang, and X. G. Jian, "Hydrophobic modification of poly(phthalazinone ether sulfone ketone) hollow fiber membrane for vacuum membrane distillation," *Journal of Membrane Science*, vol. 310, no. 1-2, pp. 20–27, 2008.

[24] D. E. Suk, T. Matsuura, H. B. Park, and Y. M. Lee, "Development of novel surface modified phase inversion membranes having hydrophobic surface-modifying macromolecule (nSMM) for vacuum membrane distillations," *Desalination*, vol. 261, no. 3, pp. 300–312, 2010.

[25] N. Tang, Q. Jia, H. Zhang, J. Li, and S. Cao, "Preparation and morphological characterization of narrow pore size distributed polypropylene hydrophobic membranes for vacuum membrane distillation via thermally induced phase separation," *Desalination*, vol. 256, no. 1–3, pp. 27–36, 2010.

[26] B. Wu, K. Li, and W. K. Teo, "Preparation and characterization of poly(vinylidene fluoride) hollow fiber membranes for vacuum membrane distillation," *Journal of Applied Polymer Science*, vol. 106, no. 3, pp. 1482–1495, 2007.

[27] Z. Jin, D. L. Yang, S. H. Zhang, and X. G. Jian, "Removal of 2,4-dichlorophenol from wasterwater by vacuum membrane distillation using hydrophobic PPESK hollow hiber membrane," *Chinese Chemical Letters*, vol. 18, no. 12, pp. 1543–1547, 2007.

[28] B. Wu, X. Tan, K. Li, and W. K. Teo, "Removal of 1,1,1-trichloroethane from water using a polyvinylidene fluoride hollow fiber membrane module: vacuum membrane distillation operation," *Separation and Purification Technology*, vol. 52, no. 2, pp. 301–309, 2006.

[29] B. Li and K. K. Sirkar, "Novel membrane and device for vacuum membrane distillation-based desalination process," *Journal of Membrane Science*, vol. 257, no. 1-2, pp. 60–75, 2005.

[30] M. Khayet and T. Matsuura, "Pervaporation and vacuum membrane distillation processes: modeling and experiments," *AIChE Journal*, vol. 50, no. 8, pp. 1697–1712, 2004.

[31] M. Khayet, K. C. Khulbe, and T. Matsuura, "Characterization of membranes for membrane distillation by atomic force microscopy and estimation of their water vapor transfer coefficients in vacuum membrane distillation process," *Journal of Membrane Science*, vol. 238, no. 1-2, pp. 199–211, 2004.

[32] J.-M. Li, Z.-K. Xu, Z.-M. Liu et al., "Microporous polypropylene and polyethylene hollow fiber membranes—part 3: experimental studies on membrane distillation for desalination," *Desalination*, vol. 155, no. 2, pp. 153–156, 2003.

[33] M. Khayet and T. Matsuura, "Preparation and characterization of polyvinylidene fluoride membranes for membrane distillation," *Industrial and Engineering Chemistry Research*, vol. 40, no. 24, pp. 5710–5718, 2001.

[34] H. Abdallah, A. F. Moustafa, A. A. AlAnezi, and H. E. M. El-Sayed, "Performance of a newly developed titanium oxide nanotubes/polyethersulfone blend membrane for water desalination using vacuum membrane distillation," *Desalination*, vol. 346, pp. 30–36, 2014.

[35] M. Safavi and T. Mohammadi, "High-salinity water desalination using VMD," *Chemical Engineering Journal*, vol. 149, no. 1–3, pp. 191–195, 2009.

[36] J.-M. Li, Z.-K. Xu, Z.-M. Liu et al., "Microporous polypropylene and polyethylene hollow fiber membranes. Part 3. Experimental studies on membrane distillation for desalination," *Desalination*, vol. 155, no. 2, pp. 153–156, 2003.

[37] C.-K. Chiam, A. Ibrahim, and R. Sarbatly, "Desalination in cross-flow vacuum membrane distillation under the negative membrane pressure difference," *Journal of Applied Sciences*, vol. 14, no. 12, pp. 1259–1264, 2014.

[38] S. Srisurichan, R. Jiraratananon, and A. G. Fane, "Mass transfer mechanisms and transport resistances in direct contact membrane distillation process," *Journal of Membrane Science*, vol. 277, no. 1-2, pp. 186–194, 2006.

[39] J. Phattaranawik and R. Jiraratananon, "Direct contact membrane distillation: effect of mass transfer on heat transfer," *Journal of Membrane Science*, vol. 188, no. 1, pp. 137–143, 2001.

[40] M. Khayet, A. O. Imdakm, and T. Matsuura, "Monte Carlo simulation and experimental heat and mass transfer in direct contact membrane distillation," *International Journal of Heat and Mass Transfer*, vol. 53, no. 7-8, pp. 1249–1259, 2010.

[41] A. M. Alklaibi and N. Lior, "Membrane-distillation desalination: status and potential," *Desalination*, vol. 171, no. 2, pp. 111–131, 2005.

[42] L. Martínez-Díez, M. I. Vázquez-González, and F. J. Florido-Díaz, "Study of membrane distillation using channel spacers," *Journal of Membrane Science*, vol. 144, no. 1-2, pp. 45–56, 1998.

[43] M. Khayet, "Membrane distillation," in *Advanced Membrane Technology and Applications*, N. N. Li, A. G. Fane, W. S. W. Ho, and T. Matsuura, Eds., pp. 297–370, John Wiley & Sons, Inc, New York, NY, USA, 2008.

[44] M. Sudoh, K. Takuwa, H. Iizuka, and K. Nagamatsuya, "Effects of thermal and concentration boundary layers on vapor permeation in membrane distillation of aqueous lithium bromide solution," *Journal of Membrane Science*, vol. 131, no. 1-2, pp. 1–7, 1997.

[45] T. Mohammadi and M. A. Safavi, "Application of Taguchi method in optimization of desalination by vacuum membrane distillation," *Desalination*, vol. 249, no. 1, pp. 83–89, 2009.

[46] S. Bandini, C. Gostoli, and G. C. Sarti, "Separation efficiency in vacuum membrane distillation," *Journal of Membrane Science*, vol. 73, no. 2-3, pp. 217–229, 1992.

[47] S. Al-Asheh, F. Banat, M. Qtaishat, and M. Al-Khateeb, "Concentration of sucrose solutions via vacuum membrane distillation," *Desalination*, vol. 195, no. 1–3, pp. 60–68, 2006.

[48] R. Bagger-Jørgensen, A. S. Meyer, C. Varming, and G. Jonsson, "Recovery of volatile aroma compounds from black currant juice by vacuum membrane distillation," *Journal of Food Engineering*, vol. 64, no. 1, pp. 23–31, 2004.